Carbazolophane Enhances the Efficiency of Thermally Activated Delayed Fluorescence in Carbene Coinage Metal Amides

Received 00th January 20xx,
Accepted 00th January 20xx

DOI: 10.1039/x0xx00000x

Indranil Sen,[a] Ondřej Mrózek,[a] Mousree Mitra,[a] Andrey Belyaev,[a] Changfeng Si,[b] Eli Zysman-Colman,[b] Jasmin Seibert,[c] Stefan Bräse,[c,d] and Andreas Steffen*[a]

Carbene coinage metal carbazolates are currently the most efficient organometallic TADF emitters. Herein we report on the photophysical influence of introducing a [2.2]paracyclophane moiety via a carbazolophane ligand instead of carbazolate, which greatly enhances the radiative rate constants by a factor of three to 1-3·10^6 s^{-1} for triplet exciton emission.

Coinage metal carbene complexes in the oxidation state +I have emerged as a versatile class of photoactive compounds within the last decade.[1-4] Unlike d^6 and d^8 metal complexes with relatively strict octahedral and square-planar structures, the d^{10} electron configuration allows for ligand coordination in various geometries, which greatly influences the nature and properties of the excited states and thus provides a high degree of photophysical tunability. Consequently, coinage metal carbenes have found myriad applications in catalysis, OLEDs, and stimulus-responsive materials.[1, 3, 5-13]

Linearly coordinated systems featuring a donor-M-acceptor (D-M-A) structure often display thermally activated delayed fluorescence (TADF), bypassing the spin-forbidden phosphorescence from the T_1 state by endothermic reverse intersystem-crossing (rISC) and subsequent $S_1 \rightarrow S_0$ emission.[7-9, 14-20] With this alternative luminescence mechanism relevant for efficient triplet exciton harvesting in device technologies, radiative rate constants k_{TADF} of 10^5-10^6 s^{-1} can be achieved that are competitive or even higher than obtained with traditional 4d/5d metal complexes that provide spin-orbit coupling (SOC) for phosphorescence.[2, 21-23]

In this regard, coinage metal carbazolates (CMCz) have gained particular attention due to their exceptional luminescence efficiency,[7-9, 14-20] and high-level DFT and transient absorption studies have clarified the details of the TADF mechanism.[19, 24-28] Typically, their lowest energy excited states are of $^{1/3}$LLCT character, of which the energy gap depends on the relative orientation of the carbene and Cz ligands. In a co-planar arrangement, these states are energetically well separated, but the ^{1}LLCT state bears significant oscillator strength for efficient radiative $S_1 \rightarrow S_0$ decay. Ligand rotation or M–N(Cz) bond bending, however, decouples the electron and hole in the $^{1/3}$LLCT states, and they become nearly isoenergetic, leading to strong spin-vibronic coupling and very facile (r)ISC processes $S_1 \leftrightarrows T_1$.

This dynamic TADF mechanism is generally very similar to that found in many efficient organic emitters.[29, 30] However, organometallic complexes can enhance the operative SOC either by coupling of S_1 and T_1 with energetically close-lying metal-to-ligand charge-transfer (MLCT) states and by the heavy atom effect, both scenarios further accelerating the (r)ISC and thus the overall efficiency of TADF. Consequently, very high k_{TADF} of up to 1-2·10^6 s^{-1} have been achieved for some selected examples of Ag and Au complexes.[8, 16, 20]

It should be noted that k_{TADF} of up to 1·10^6 s^{-1} have also been reported for a few organic TADF emitters by, e.g., designing through-space $^{1/3}$CT states that feature very small $\Delta E(S_1\text{-}T_1)$ or by introduction of intermediate triplet states fostering rISC.[25,31] However, one has to bear in mind that this comes at the price of reducing the oscillator strength of the $S_1 \rightarrow S_0$ transition, which implies a natural limit of k_{TADF} for this particular approach.

In order to find structural design principles for efficient emitters, we were curious whether k_{TADF} in linear CMCz as established TADF systems could be enhanced by reducing $\Delta E(S_1\text{-}T_n)$ to assist the rISC without sacrificing the oscillator strength of the emitting S_1 state. A suitable moiety for this purpose appears

[a] Department of Chemisty and Chemical Biology, TU Dortmund University, Otto-Hahn-Str. 6, 44227 Dortmund, Germany. Email: andreas.steffen@tu-dortmund.de
[b] Organic Semiconductor Centre, EaStCHEM School of Chemistry, University of St Andrews, St Andrews, Fife, UK, KY16 9ST.
[c] Institute of Organic Chemistry, Karlsruhe Institute of Technology (KIT), Fritz-Haber-Weg 6, Karlsruhe, Germany.
[d] Institute of Biological and Chemical Systems – Functional Molecular Systems (IBCS-FMS), Karlsruhe Institute of Technology (KIT), Hermann-von-Helmholtz-Platz 1, Eggenstein-Leopoldshafen, Germany

Electronic Supplementary Information (ESI) available: [details of any supplementary information available should be included here]. See DOI: 10.1039/x0xx00000x

to be indolo[2.2]paracyclophane (carbazolophane, Czp) as a derivative of Cz, which has been reported to be a very potent donor moiety in organic TADF systems.[32, 33] Also, Czp provides greater steric encumbrance that would still allow for ligand rotation to some degree to decrease $\Delta E(^{1/3}LLCT)$, but should avoid 90° conformations, which are associated with an absence of oscillator strength for fluorescence and hence slow k_{TADF}, and consequently increase the probability of the vertical transition. Treatment of [MCl(cAAC^{Et})] (M = Cu, Ag, Au; cAAC = cyclic (alkyl)(amino)carbene) with HCzp in the presence of KHMDS provides facile access to **1-3**, of which yellow-to-green single crystals suitable for X-ray diffraction studies were obtained in good yields of 41-54% either from THF/n-pentane mixture (**1**) or cooling of saturated toluene solutions to -40 °C (**2** and **3**) (Scheme 1). The introduction of the paracyclophane motif as a steric modification of Cz has only negligible influence on the ground state structures. The Czp complexes **1**-**3** exhibit a nearly linear coordination environment with N–M–C^{carbene} angles of ~175°, and the cAAC^{Et} and Czp ligands adopt a co-planar arrangement. The M–C^{carbene} and M–N bond lengths increase in the order **1** (Cu) < **3** (Au) < **2** (Ag), resulting in N···C^{carbene} distances of 3.7 (**1**), 4.1 (**2**) and 4.0 (**3**) Å, which are also very close to those found for previously reported group 11 [M(Cz)(cAAC)] complexes.[8, 9, 18]

UV/vis absorption spectra of **1-3** in 2-MeTHF show broad low energy MLCT/LLCT bands between 400-450 nm with low extinction coefficients of ε = 1,500-7,500 M^{-1} cm^{-1}, that increase in the order Ag (**2**) < Cu (**1**) < Au (**3**), which is supported by TD-DFT calculations (Figure 1, and Supporting Information). Negative solvatochromism with shifts of up to ca. 4,500 cm^{-1} between nonpolar n-pentane and polar acetonitrile is observed for the $S_0 \rightarrow S_1$ transitions, which suggests that the ground state in **1-3** is much more polar than the ^{1}LLCT excited state (Figures S13-S15).[34]

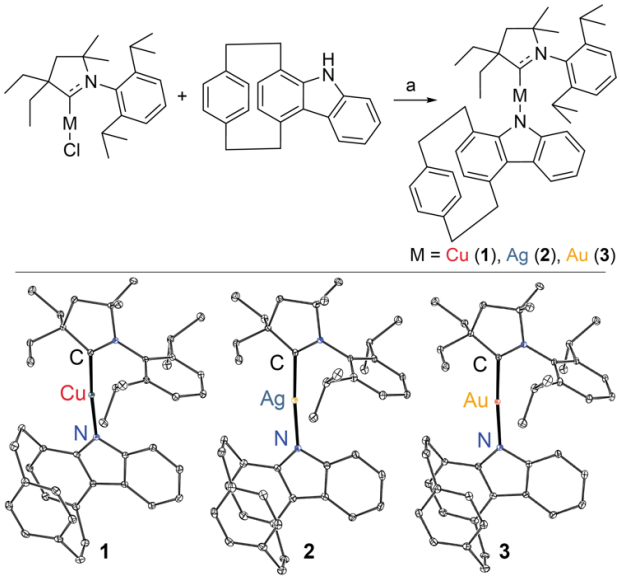

Scheme 1. Top: synthesis of target carbazolate complexes **1-3**; a = KHMDS/THF. Bottom: ORTEP view of **1-3**, thermal ellipsoids are drawn at the 30 % probability level, hydrogens and solvent molecules are omitted for clarity. Selected bond lengths (Å) and angles (°) for **1** (M = Cu), **2** (M = Ag) and **3** (M = Au), respectively: M–C 1.8773(11), 2.057(2), 1.9771(1); M–N 1.8621(10), 2.058(2), 2.0213(1); C–M–N 174.90(5), 174.69(9), 175.82(1).

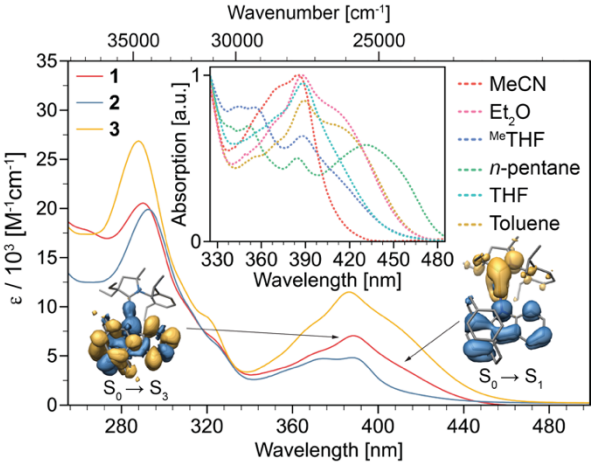

Figure 1. Experimental UV/vis absorption spectra of **1-3** in 2-MeTHF and electron density differences of the ^{1}LLCT and ^{1}LC transitions of [Cu(Czp)(cAAC^{Et})] (**1**) (D3(BJ)-PBE0/ZORA/def2-SVP/CPCM). Inset: negative solvatochromism of the ^{1}LLCT band of **1**.

The more structured band between 330-400 nm exhibits higher extinction coefficients of 7,100 (**1**), 4,800 (**2**) and 11,500 (**3**) M^{-1} cm^{-1} and originates from a ^{1}LC(Czp) transition with MLCT admixture. We note that the offset of the ^{1}LLCT band and the absorption maximum of the ^{1}LC transition of **1** are bathochromically shifted in comparison to [Cu(Cz)(cAAC^{Et})] ($\lambda_{offset/max}$ = 450 and 390 nm vs 425 and 370 nm) due to the paracyclophane motif of the Czp ligand.[9] At higher energies in the UV, intense ($\varepsilon \geq$ 20,000 M^{-1} cm^{-1}) $\pi \rightarrow \pi^*$ transitions of the arene moieties are observed.

All compounds show intense photoluminescence with lifetimes of a few hundred nanoseconds in solution at room temperature (Table 1 and Figure 2). Minor positive solvatochromism is displayed in the shifts of λ_{max}(em), although the excited CT state is less polar than the ground state (see above, Figures S16-S18). This effect appears to arise from small solvent-dependent differences in the structural reorganization upon photoexcitation because the onsets of the emission are solvent independent.

Table 1. Luminescence properties of **1-3** in various solvents at room temperature.

	Medium	λ_{max} / nm	[a] τ_{av} / ns	ϕ_{PL}	[b] k_{TADF} / s^{-1}	[c] k_{nr} / s^{-1}
1	*n*-pentane	530	1190	0.52	4.4×10^5	4.0×10^5
	toluene	539	728	0.80	1.1×10^6	2.8×10^5
	Et_2O	546	856	0.85	9.9×10^5	1.8×10^5
	2-MeTHF	552	534	0.50	9.4×10^5	9.4×10^5
	MeCN	553	293	0.29	9.9×10^5	2.4×10^6
2	*n*-pentane	553	110	0.36	3.3×10^6	5.8×10^6
	toluene	569	183	0.25	1.4×10^6	4.1×10^6
	Et_2O	582	118	0.11	9.3×10^5	7.5×10^6
	2-MeTHF	575	146	0.06	4.1×10^5	6.4×10^6
	MeCN	584	104	<0.01	$\leq 9.6\times10^4$	$\geq 9.5\times10^6$
3	*n*-pentane	541	199	0.54	2.7×10^6	2.3×10^6
	toluene	550	149	0.42	2.8×10^6	3.9×10^6
	Et_2O	557	397	0.25	6.3×10^5	1.9×10^6
	2-MeTHF	562	158	0.18	1.1×10^6	5.2×10^6
	MeCN	569	83	0.07	8.4×10^5	1.1×10^7

[a] For multiexponential decays, the amplitude averaged lifetimes are given (see also Supporting Information). [b] $k_{TADF} = \phi_{PL}/\tau$. [c] $k_{nr} = (1-\phi_{PL})/\tau$.

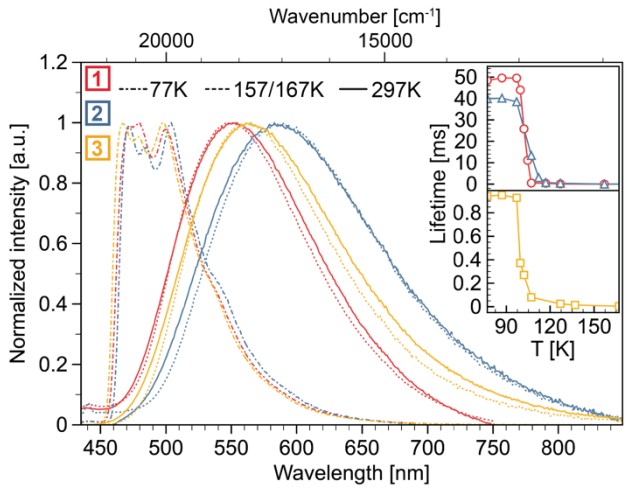

Figure 2. Normalized emission spectra (λ_{ex} = 380 nm) of **1-3** in fluid 2-MeTHF at 297 (solid) and 157/167 K (dotted), and in frozen 2-MeTHF optical glass at 77 K (dashed). Inset: temperature-dependent emission lifetimes of **1-3**.

The emission energies in the green to orange region of the electromagnetic spectrum are shifted bathochromically along the series Cu > Au > Ag.

Complex **1** is the most efficient emitter with the highest photoluminescence quantum yields ϕ_{PL}, reaching values of up to 0.85 in Et_2O, and concomitant high k_r 0.9-1.1·10^6 s^{-1} (Table 1). Interestingly, k_r is reduced to 4.4·10^5 s^{-1} in *n*-pentane. The comparison of **1** with previously reported [Cu(Cz)(cAAC^{Et})] (k_r = 3·10^5 s^{-1} in 2-MeTHF) is very insightful and shows that the Czp moiety enhances k_r by a factor of 3.[9] The ϕ_{PL} are significantly reduced for the silver and gold congeners **2** and **3**, which is a result of enhanced non-radiative decay in comparison to **1** and not due to reduced k_r (Table 1). Actually, the k_r of **2** and **3** are very high in nonpolar toluene and *n*-pentane with values of up to 3.3·10^6 (**2**) and 2.8·10^6 s^{-1} (**3**), and are found to be among the highest values ever reported for organometallic triplet exciton emitters.[2-4, 7-9, 11, 13-16, 18-20, 23, 35]

Such high k_r in D-A compounds are typically the result of an efficient TADF process. Further indication that the excited state decays to the ground state from the S_1 state is provided by the high k_{nr}, excluding non-radiative decay from T_1 as that process would be much slower due to its spin-forbidden nature.

Indeed, time-resolved VT measurements of **1-3** in polar 2-MeTHF show an increase of the radiative lifetimes by several orders of magnitude into the millisecond domain at 77 K, typical for a change of the emission mechanism from TADF to phosphorescence (Figure 2). The temperature-dependent spectral evolution reveals a thermal equilibrium between the $^{1/3}$LLCT states because the emission band remains broad until the glass transition temperature of the solvent, with very small estimated energy gaps of $\Delta E(^{1/3}LLCT)$ = 130 cm^{-1} (16 meV) (**1**), 280 cm^{-1} (35 meV) (**2**) and 210 (26 meV) (**3**). However, a vibrational progression and hypsochromic emission shift are observed in the frozen glassy matrix at 77 K, originating from a ^{3}LC(Czp) state. Apparently, the solvent molecules cannot re-orient to acknowledge the change in the permanent dipole moment of the complex upon photoexcitation, which shifts the ^{3}LLCT state energetically above the ^{3}LC state. Noteworthy, the ^{3}LC(Czp) state is lower in energy by 2,000 cm^{-1} (0.25 eV) than the ^{3}LC(Cz) in related coinage metal complexes (λ_{em} = 420 nm) and exhibits a much greater spectral overlap with the $^{1/3}$LLCT states. In addition, we estimate small energy gaps of $\Delta E(^3LC/^{1/3}LLCT)$ = 1050 cm^{-1} (130 meV) (**1**), 1540 cm^{-1} (190 meV) (**2**) and 1430 cm^{-1} (180 meV) (**3**) from the emission onsets, which indicates strong vibrational coupling of these states to facilitate efficient rISC for TADF.

In conclusion, exchanging the carbazolate ligand for carbazolophane in coinage metal carbene complexes shifts the steady state equilibrium between the excited states involved in the TADF process towards the ^{1}LLCT state by reducing $\Delta E(^{1/3}LLCT)$ and opening another rISC channel via the ^{3}LC(Czp) state. In addition, the steric demand of the [2.2]paracyclophane moiety apparently avoids dihedral angles between the ligands close to 90° with little oscillator strength for the transition $S_1 \rightarrow S_0$. Consequently, very high k_{TADF} in nonpolar solvents of 1.1-3.3·10^6 s^{-1} are obtained, which are greatly increased compared to the analogous Cz complexes. Further studies on the excited state dynamics are currently underway.

Conflicts of interest

There are no conflicts to declare.

Notes and references

Financial support by the Deutsche Forschungsgemeinschaft (DFG STE1834/4-2) is gratefully acknowledged. C.S. thanks the China Scholarship Council (201806890001). The authors gratefully acknowledge the computing time provided on the Linux HPC cluster at Technical University Dortmund (LiDO3), partially funded in the course of the Large-Scale Equipment Initiative by the German Research Foundation (DFG) as project 271512359.

1. H. Amouri, *Chem. Rev.*, 2023, **123**, 230-270.
2. A. Steffen and B. Hupp, in *Comprehensive Coordination Chemistry III*, eds. E. C. Constable, G. Parkin and L. Que Jr, Elsevier, Oxford, 2021, DOI: https://doi.org/10.1016/B978-0-12-409547-2.14753-5, pp. 466-502.
3. J. Hossain, R. Akhtar and S. Khan, *Polyhedron*, 2021, **201**, 115151.
4. R. Jazzar, M. Soleilhavoup and G. Bertrand, *Chem. Rev.*, 2020, **120**, 4141-4168.
5. E. A. Martynova, V. A. Voloshkin, S. G. Guillet, F. Bru, M. Beliš, K. Van Hecke, C. S. J. Cazin and S. P. Nolan, *Chem. Sci.*, 2022, **13**, 6852-6857.
6. N. V. Tzouras, E. A. Martynova, X. Ma, T. Scattolin, B. Hupp, H. Busen, M. Saab, Z. Zhang, L. Falivene, G. Pisano, K. Van Hecke, L. Cavallo, C. S. J. Cazin, A. Steffen and S. P. Nolan, *Chem. Eur. J.*, 2021, **27**, 11904-11911.
7. S. Shi, M. C. Jung, C. Coburn, A. Tadle, D. Sylvinson M. R, P. I. Djurovich, S. R. Forrest and M. E. Thompson, *J. Am. Chem. Soc.*, 2019, **141**, 3576–3588.
8. R. Hamze, S. Shi, S. C. Kapper, D. S. Muthiah Ravinson, L. Estergreen, M.-C. Jung, A. C. Tadle, R. Haiges, P. I. Djurovich, J. L. Peltier, R. Jazzar, G. Bertrand, S. E. Bradforth and M. E. Thompson, *J. Am. Chem. Soc.*, 2019, **141**, 8616–8626.

9. R. Hamze, J. L. Peltier, D. Sylvinson, M. Jung, J. Cardenas, R. Haiges, M. Soleilhavoup, R. Jazzar, P. I. Djurovich, G. Bertrand and M. E. Thompson, *Science*, 2019, **363**, 601–606.
10. B. Hupp, J. Nitsch, T. Schmitt, R. Bertermann, K. Edkins, F. Hirsch, I. Fischer, M. Auth, A. Sperlich and A. Steffen, *Angew. Chem. Int. Ed.*, 2018, **57**, 13671–13675.
11. M. Elie, F. Sguerra, F. Di Meo, M. D. Weber, R. Marion, A. Grimault, J.-F. Lohier, A. Stallivieri, A. Brosseau, R. B. Pansu, J.-L. Renaud, M. Linares, M. Hamel, R. D. Costa and S. Gaillard, *ACS Appl. Mater. Interfaces*, 2016, **8**, 14678–14691.
12. J. Foller, C. Ganter, A. Steffen and C. M. Marian, *Inorg. Chem.*, 2019, **58**, 5446-5456.
13. J. Nitsch, F. Lacemon, A. Lorbach, A. Eichhorn, F. Cisnetti and A. Steffen, *Chem. Commun.*, 2016, 2932–2935.
14. R. Tang, S. Xu, T.-L. Lam, G. Cheng, L. Du, Q. Wan, J. Yang, F.-F. Hung, K.-H. Low, D. L. Phillips and C.-M. Che, *Angew. Chem. Int. Ed.*, 2022, **61**, e202203982.
15. A. Ruduss, B. Turovska, S. Belyakov, K. A. Stucere, A. Vembris, G. Baryshnikov, H. Ågren, J.-C. Lu, W.-H. Lin, C.-H. Chang and K. Traskovskis, *ACS Appl. Mater. Interfaces*, 2022, **14**, 15478-15493.
16. C. N. Muniz, J. Schaab, A. Razgoniaev, P. I. Djurovich and M. E. Thompson, *J. Am. Chem. Soc.*, 2022, **144**, 17916-17928.
17. A. Ying, Y.-H. Huang, C.-H. Lu, Z. Chen, W.-K. Lee, X. Zeng, T. Chen, X. Cao, C.-C. Wu, S. Gong and C. Yang, *ACS Appl. Mater. Interfaces*, 2021, **13**, 13478-13486.
18. A. S. Romanov, S. T. E. Jones, Q. Gu, P. J. Conaghan, B. H. Drummond, J. Feng, F. Chotard, L. Buizza, M. Foley, M. Linnolahti, D. Credgington and M. Bochmann, *Chem. Sci.*, 2020, **11**, 435-446.
19. M. Gernert, L. Balles-Wolf, F. Kerner, M. U. L. U, A. Schmiedel, M. Holzapfel, C. M. Marian, J. Pflaum, C. Lambert and A. Steffen, *J. Am. Chem. Soc.*, 2020, **142**, 8897-8909.
20. F. Chotard, V. Sivchik, M. Linnolahti, M. Bochmann and A. S. Romanov, *Chem. Mater.*, 2020, **32**, 6114-6122.
21. G. Hong, X. Gan, C. Leonhardt, Z. Zhang, J. Seibert, J. M. Busch and S. Bräse, *Adv. Mater.*, 2021, **33**, 2005630.
22. O. S. Wenger, *J. Am. Chem. Soc.*, 2018, **140**, 13522–13533.
23. L. Bergmann, D. M. Zink, S. Bräse, T. Baumann and D. Volz, in *Topics in Current Chemistry*, Springer Berlin, Heidelberg, 2016, vol. 374.
24. E. J. Taffet, Y. Olivier, F. Lam, D. Beljonne and G. D. Scholes, *J. Phys. Chem. Lett.*, 2018, **9**, 1620–1626.
25. T. J. Penfold, E. Gindensperger, C. Daniel and C. M. Marian, *Chem. Rev.*, 2018, **118**, 6975–7025.
26. C. R. Hall, A. S. Romanov, M. Bochmann and S. R. Meech, *J. Phys. Chem. Lett.*, 2018, **9**, 5873–5876.
27. J. Föller and C. M. Marian, *J. Phys. Chem. Lett.*, 2017, **8**, 5643–5647.
28. S. Thompson, J. Eng and T. J. Penfold, *J. Chem. Phys.*, 2018, **149**, 014304.
29. K. Ye, L. Cao, D. M. E. van Raamsdonk, Z. Wang, J. Zhao, D. Escudero and D. Jacquemin, *Beilstein J. Org. Chem.*, 2022, **18**, 1435-1453.
30. M. Y. Wong, E. Zysman-Colman, *Adv. Mater.*, 2017, **29**, 1605444.
31. a) J. M. Kaminski, A. Rodríguez-Serrano, F. Dinkelbach, H. Miranda-Salinas, A. P. Monkman and C. M. Marian, *Chem. Sci.*, 2022, **13**, 7057-7066; b) E. Zysman-Colman, *Nat. Photonics*, 2020, **14**, 593–594.
32. A. K. Gupta, Z. Zhang, E. Spuling, M. Kaczmarek, Y. Wang, Z. Hassan, I. D. W. Samuel, S. Bräse and E. Zysman-Colman, *Materials Advances*, 2021, **2**, 6684-6693.
33. N. Sharma, E. Spuling, Cornelia M. Mattern, W. Li, O. Fuhr, Y. Tsuchiya, C. Adachi, S. Bräse, I. D. W. Samuel and E. Zysman-Colman, *Chem. Sci.*, 2019, **10**, 6689-6696.
34. C. Reichardt, *Chem. Rev.*, 1994, **94**, 2319-2358.
35. M. J. Leitl, D. M. Zink, A. Schinabeck, T. Baumann, D. Volz and H. Yersin, in *Topics in Current Chemistry*, Springer Berlin, Heidelberg, 2016, vol. 374.